High-Resolution Imaging of Antibodies by Tapping-Mode Atomic Force Microscopy: Attractive and Repulsive Tip-Sample Interaction Regimes

Alvaro San Paulo and Ricardo García
Instituto de Microelectrónica de Madrid, Consejo Superior de Investigaciones Científicas, 28760 Tres Cantos, Madrid, Spain

ABSTRACT A force microscope operated with an amplitude modulation feedback (usually known as tapping-mode atomic force microscope) has two tip-sample interaction regimes, *attractive* and *repulsive.* We have studied the performance of those regimes to imaging single antibody molecules. The attractive interaction regime allows determination of the basic morphologies of the antibodies on the support. More importantly, this regime is able to resolve the characteristic Y-shaped domain structure of antibodies and the hinge region between domains. Imaging in the repulsive interaction regime is associated with the irreversible deformation of the molecules. This causes a significant loss in resolution and contrast. Two major physical differences distinguish the repulsive interaction regime from the attractive interaction regime: the existence of tip-sample contact and the strength of the forces involved.

INTRODUCTION

Atomic force microscopy (AFM) is widely used to image biomolecules, from whole cells down to smaller structures, such as membranes, proteins, and nucleic acids (see reviews by Hansma and Hoh, 1994; Henderson, 1994; Bustamante et al., 1997). High-resolution imaging of individual proteins physisorbed to surfaces is one of the most challenging tasks to date. The lateral forces present in contact mode experiments usually sweep weakly adsorbed molecules during scanning. Additionally, normal forces could also deform or distort the molecule. Dynamic AFM modes, tapping-mode AFM among them, were developed to improve lateral resolution and minimize sample distortion or damage (Martin et al., 1987; Hansma and Hoh, 1994; Putman et al., 1994; Anselmatti et al., 1994). A large variety of biomolecules, cells, and molecule-molecule interactions have been studied by tapping-mode AFM in air and liquid environments (Henderson, 1994; Fritz et al., 1995, 1997; Valle et al., 1996; Muñoz-Botella et al., 1996; Samori, 1998; Margeat et al., 1998). However, in most cases tapping-mode images of individual proteins are unable to reveal the fragments or subunits forming the molecule. Several factors such as the tip-sample convolution, the very low compliance of small molecules, or the deformation induced by the tip-sample forces during impact could contribute to limit the resolution.

The cantilever motion in dynamic AFM is fairly complex. Furthermore, a thorough understanding of the tip-sample interaction in tapping-mode AFM is still emerging (Anczykowski et al., 1996; Tamayo and García, 1996, 1997; Kühle et al., 1997; Haugstad and Jones, 1999; Lantz et al., 1999). Recently, a theoretical description of an AFM operated with an amplitude modulation feedback, usually known as tapping-mode AFM, has revealed the existence of two interaction regimes, *attractive* and *repulsive* (García and San Paulo, 1999a). Experimental evidence of the existence of those regimes has been provided by measuring amplitude curves on mica and semiconductor samples (García and San Paulo, 1999b).

In the attractive interaction regime a net attractive force dominates the amplitude reduction, while in the repulsive interaction regime a net repulsive force controls the cantilever dynamics. In many cases the attractive interaction regime is performed in the absence of tip-sample contact. In the repulsive interaction regime, long-range attractive and short-range repulsive forces control the cantilever motion. This regime implies tip-sample contact at one end of the oscillation. It is likely that if there is sample distortion or damage it should happen precisely during the contact between tip and sample.

The contact time depends on the mechanical properties of the sample. For example, a sample of Young's modulus of 1 GPa could have contact times of ~0.2–0.3 T, where T is the period of the oscillation. The contact time increases with decreasing Young's modulus. AFM measurements of the elastic modulus of biomolecules and cells show a wide range of values from 1 kPa for human platelets (Radmacher et al., 1996) to 1 GPa for antibodies at low temperatures (Han et al., 1995). Experiments performed on samples with very low elastic moduli could have contact times close to T.

In this study we investigate the implications of the existence of two interaction regimes in tapping-mode AFM imaging of single biomolecules. Specifically, we want to establish whether the attractive interaction regime due to the absence of tip-sample contact represents an advantage in terms of resolution and contrast. We have chosen antibody molecules (anti-human serum albumin) for this purpose. The simplest antibody molecules (~150 kD) are made of three fragments, two separate and identical fragments with active sites for antigen-binding Fab, and one Fc fragment.

Received for publication 26 July 1999 and in final form 3 December 1999.
Address reprint requests to Dr. Ricardo García, Instituto de Microelectrónica de Madrid, CSIC, Isaac Newton 8, 28760 Tres Cantos, Madrid, Spain. Tel.: 34-91-806-07-00; Fax: 34-91-806-07-01; E-mail: rgarcia@imm.cnm.csic.es.

0006-3495/00/03/1599/07 $2.00

The three-dimensional structure resembles a T- or Y-shaped conformation. This conformation gives them a distinctive morphology (see schematic drawing in Fig. 1). The ability to distinguish this morphology is used to evaluate the advantages/limitations of each interaction regime. Additionally, the study of the antibody/antigen interaction by force microscopy is receiving considerable attention (Dammer et al., 1996; Allen et al., 1997; Willemsen et al., 1998). Those studies could benefit from new developments in the imaging of biomolecules.

MATERIALS AND METHODS

Anti-human serum albumin, a-HSA (Sigma Chemical, St. Louis, MO) were used without further purification. The stock solution (1 mg/ml) was diluted to a concentration of 1 μg/ml or 1.3×10^{-8} M. A 10-μl drop of the solution was deposited onto freshly cleaved ruby mica supports (Goodfellow, Cambridge, UK) and left to incubate for 30 s. Then the sample was rinsed with deionized water and dried N_2 gas.

The antibodies were imaged with a commercial instrument (Nanoscope III; Digital Instruments, Santa Barbara, CA). Single-beam silicon cantilevers (Pointprobe, Nanosensors, Wetzlar-Blankenfeld, Germany) with spring constants in the 25–50 N/m range were used to perform the experiments. The cantilever was oscillated at its free resonance frequency (250–350 kHz, depending on the cantilever) with a free amplitude A_0 in the 5–10 nm range. All the experiments were performed in air at room temperature and at a relative humidity of ~40%. The images were obtained by scanning the cantilever tip in a raster fashion across the sample while keeping the oscillation amplitude at a fixed value, set point amplitude (A_{sp}). The images were recorded at a line frequency of 2 Hz (512×512 pixels).

Amplitude dependence on tip-sample separation curves (amplitude curves) were obtained by approaching the tip toward the sample from a distance with negligible tip-sample interaction. The change of the oscillation amplitude was recorded as the tip-sample distance was modified. To minimize tip and/or sample damage during data acquisition, the tip excursion was stopped when the amplitude was reduced by a factor 3 with respect to the free oscillation amplitude. The curves were taken at 2 Hz with a scan size in the 10–50 nm range. To determine the maximum tip-sample force as a function of the oscillation amplitude, we have simulated the dynamic response of the cantilever-tip ensemble following the model proposed by the authors (García and San Paulo, 1999a).

RESULTS

Amplitude curves are critical to identify whether the imaging is performed in the attractive or repulsive interaction regimes. Theoretical simulations show that the amplitude decreases with tip-sample separation; however, at some distance a sudden jump in the amplitude is observed. This steplike discontinuity marks the transition between a cantilever motion dominated by long-range attractive forces to a motion controlled by short-range repulsive forces (García and San Paulo, 1999a).

Fig. 2 shows the amplitude curve obtained in a region of the support free from molecules. The curve was obtained before the imaging of the antibodies. A steplike discontinuity of 0.7 nm separates the interaction regimes. The operation of the AFM in a given regime is controlled by the feedback or set point amplitude, A_{sp}. In this case, A_{sp} values >4.8 nm imply an operation in the attractive regime, while values <3.8 nm set the cantilever in a repulsive regime operation. Amplitude values in the 3.8–4.8 nm interval are compatible with both regimes and most likely would produce severe instabilities. Fig. 2 also shows that each regime implies a different range of tip-sample separations. Amplitude curves similar to the one shown in Fig. 2 could also be obtained on top of a molecule. However, we have avoided it for reasons that will become evident below.

Fig. 3 shows a typical tapping-mode AFM image of the a-HSA molecules. The image was obtained in the attractive interaction regime. A careful inspection of several images as the one depicted in Fig. 3 reveals that the molecules show four basic morphologies. Some molecules appear to have a single domain with a lateral size (longest axis) of ~18 nm. Other molecules appear to be made of two roughly equivalent domains of ~10 nm across. The third morphology shows the antibodies with two domains, one large (~11 nm) and the other small (~8 nm). Finally, some molecules appear to be made of three roughly identical domains of ~8 nm across. Those antibodies have an overall morphology that resembles the characteristic Y-shaped conformation of the simplest antibody molecule. Fig. 4 shows a high-resolution image of each morphology.

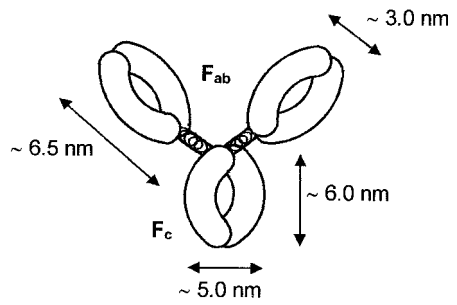

FIGURE 1 Schematic drawing of the a-HSA molecule showing the Fab arms and the Fc arm.

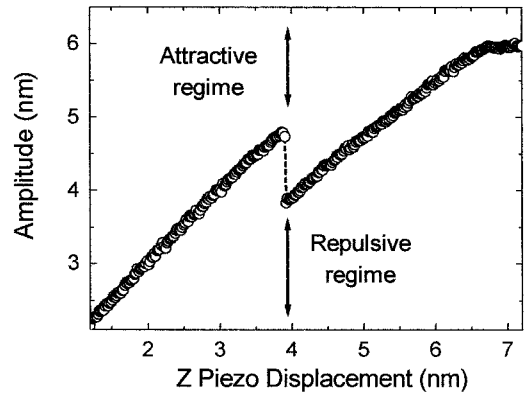

FIGURE 2 Amplitude dependence on tip-sample separation (amplitude curve). The curve was obtained on a mica region free from antibodies. The steplike discontinuity separates attractive and repulsive interaction regimes. $A_0 = 6$ nm, $f = f_0 = 259$ kHz.

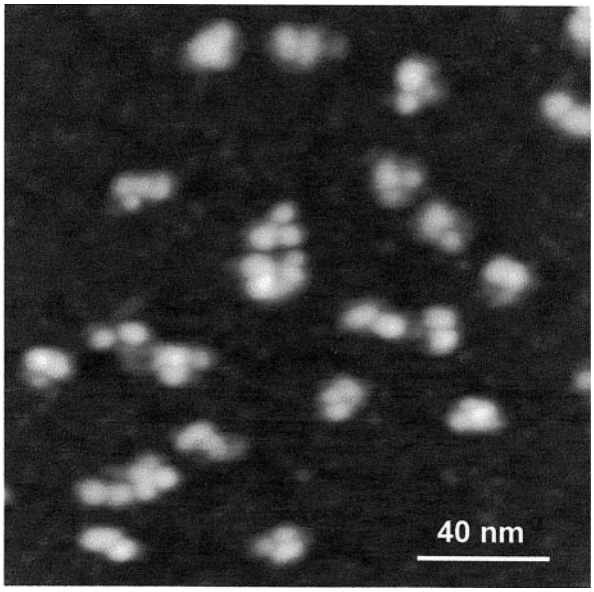

FIGURE 3 Tapping-mode AFM image (attractive interaction regime) of several antibodies. The molecules show several morphologies according to the orientation of the domains with respect to the support. Several molecules show the characteristic Y shape of antibodies. This topography is consistent with the three domains lying flat on the support. The image was obtained in air and at room temperature. $A_0 = 5$ nm, $A_{sp} = 4.3$ nm, $f = f_0 = 259$ kHz.

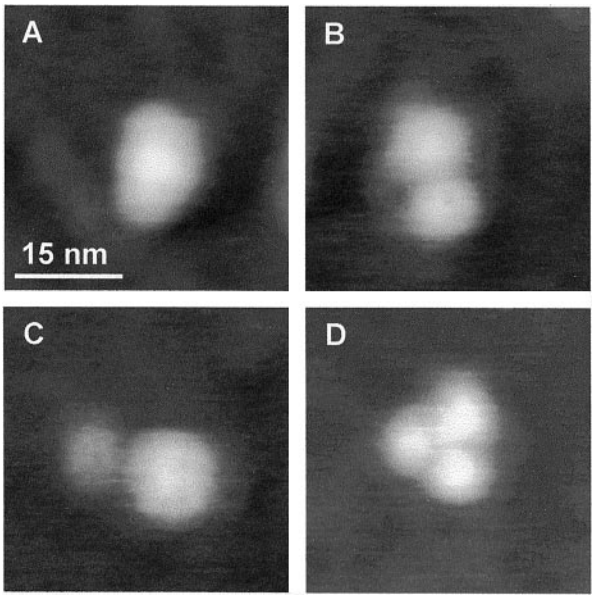

FIGURE 4 Characteristic morphologies of antibodies on mica. (*A*) Single-domain morphology of an antibody. $A_0 = 5$ nm, $A_{sp} = 2.5$ nm, $f = f_0 = 263$ kHz. (*B*) Two-domain morphology. $A_0 = 5$ nm, $A_{sp} = 2.5$ nm, $f = f_0 = 263$ kHz. (*C*) Two-unequal-domain morphology. $A_0 = 6$ nm, $A_{sp} = 3.5$ nm, $f = f_0 = 263$ kHz. (*D*) Y-shape or three-domain morphology. $A_0 = 6$ nm, $A_{sp} = 3.5$ nm, $f = f_0 = 253$ kHz. All images have been obtained in the attractive interaction regime. Image size, 40×40 nm^2.

Given the known three-dimensional morphology and size of antibodies (Silverton et al., 1977) it is tempting to associate the observed topographies with the orientation of the antibodies on the support. In this way, Fig. 4 *A* would be consistent with the antibody resting on the Fab fragments, while the Fc protrudes from the surface. Fig. 4 *B* would likely represent the opposite situation: the antibody rests on the Fc fragment while the Fab arms stick out of the surface. The molecule could also have one of the Fab arms and the Fc domain attached to the support while the other Fab arm protrudes from the surface. An AFM image of this antibody would produce an image like the one shown in Fig. 4 *C*. Finally, the Y-shaped morphology shown in Fig. 4 *D* would be consistent with the three fragments lying flat on the support. This is also supported by the observation that molecules showing this topography show the lowest apparent height (~1.5 nm).

The different topographies are probably a consequence of the nonspecific nature of adhesion on mica. Within each morphology, the lateral and vertical dimensions of the antibodies show a small variability from molecule to molecule due to the flexibility of the hinge region connecting the Fab arm with the Fc domain. For molecules showing a Y shape the small differences in the lateral dimension of the Fab or Fc domains by AFM (~8 nm) and x-ray and transmission electron microscopy measurements (6–7 nm) are mostly attributed to the finite size of the tip (nominal tip radius in the 5–15 nm range).

Next, we have devised an experiment to evaluate the performance of each interaction regime for imaging biomolecules. First a region containing several antibodies is imaged in the attractive interaction regime. A molecule showing the Y-shaped morphology is selected and an image is recorded. Then the set point amplitude is lowered to reach the repulsive interaction regime and the molecule is imaged. Finally, the amplitude is returned to its initial value (the tip is withdrawn) and the molecule is imaged again in the attractive interaction regime.

Fig. 5 shows a sequence of images of the same molecule. To better estimate the topographic changes, the corresponding cross-sections along the dashed lines are also shown. In the attractive regime the molecule shows three domains (Fig. 5 *A*). The overall shape and lateral dimensions of the molecule are in fairly good agreement with the expected image of an antibody. Furthermore, the hinge regions connecting the Fc fragment with the Fab arms are clearly resolved.

The image obtained in the repulsive interaction regime shows a jagged topography with no clear evidence of the domain structure. Two major peaks are still present in the cross-section (Fig. 5 *D*). However, those peaks fade away after repeated imaging in the repulsive regime. Fig. 5 *E* shows an image of the molecule obtained in the attractive interaction regime after the molecule was imaged in the repulsive interaction regime. The Y-shaped conformation is completely lost. The molecule shows a globular structure

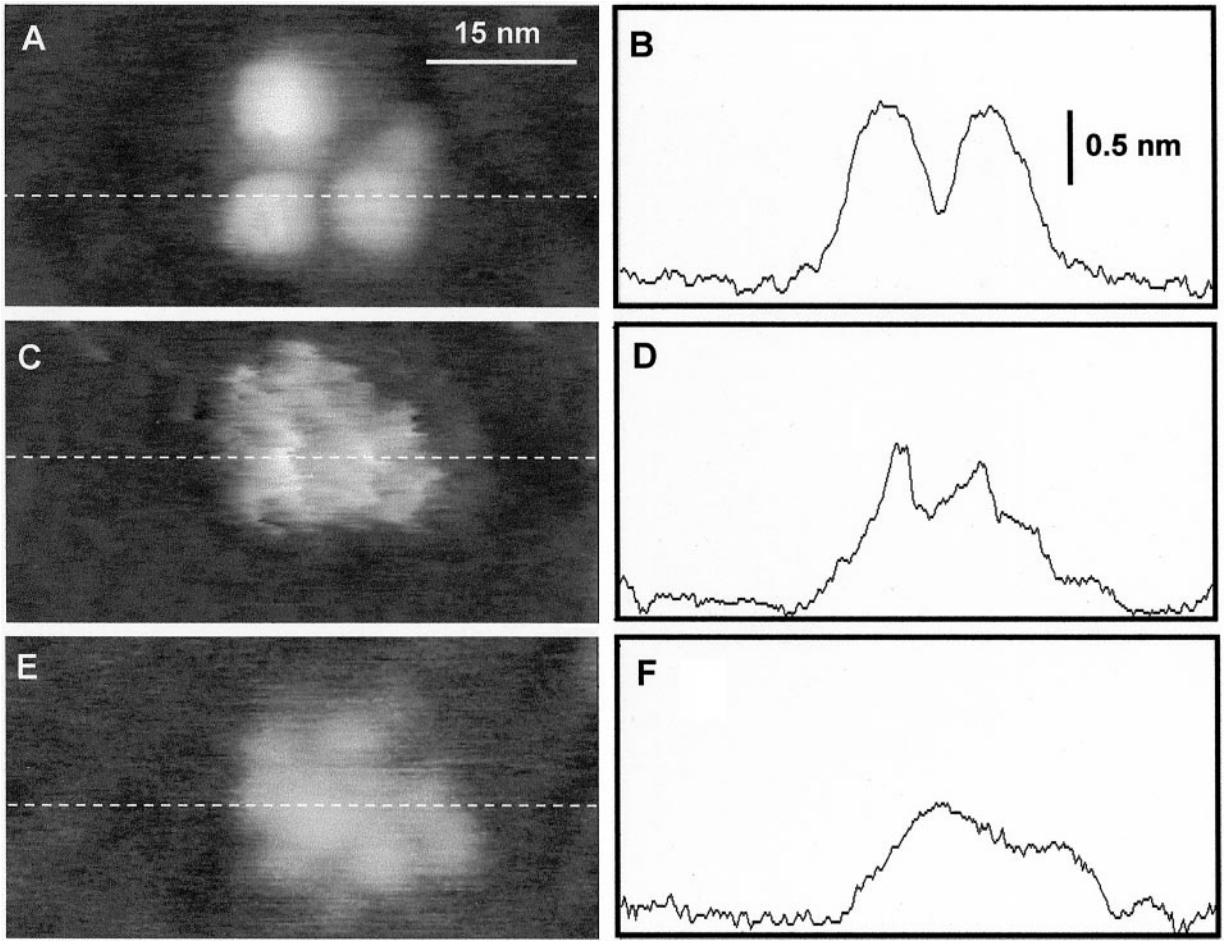

FIGURE 5 (*A*) High-resolution tapping-mode AFM image (attractive interaction regime) of a single a-HSA molecule. The three fragments and the hinge regions are clearly resolved. $A_{sp} = 5.9$ nm. (*B*) Cross-section along the dashed line in (*A*). (*C*) The same molecule imaged in the repulsive interaction regime, $A_{sp} = 2.8$ nm. (*D*) Cross-section along dashed line in (*C*). (*E*) Image of the molecule in the attractive interaction regime after repeated imaging in the repulsive regime, $A_{sp} = 5.9$ nm. The comparison between (*B*) and (*F*) cross-sections reveals the changes in the topography of the molecule after it was imaged in the repulsive interaction regime. $A_0 = 6$ nm and $f = f_0 = 259$ kHz in all cases.

with several minor domains (up to six can be counted). The apparent height of the molecule has been reduced by a factor of two with respect to the initial height (Fig. 5 *B*).

DISCUSSION AND CONCLUSIONS

Several factors could contribute to explain the observed topographic changes after repulsive interaction regime imaging. Tip-sample interaction forces in the repulsive interaction regime could have changed the orientation of the molecule with respect to the support. Alternatively, tip-sample forces could produce some irreversible modification in the molecules.

To distinguish between orientational changes and irreversible modifications, we have measured the height difference of several molecules before and after those molecules have been imaged in the repulsive interaction regime. First, 40 molecules that showed a Y- shaped morphology were selected from images taken in the attractive interaction regime. For each of them the height at its maximum was recorded. Then, the same molecules were imaged in the repulsive interaction regime. Finally, the molecules were imaged again in the attractive interaction regime. Their respective maximum height was also measured. After those measurements we were able to determine the height difference before and after the molecule was imaged in the repulsive interaction regime. The histogram shows that after taking the images in the repulsive interaction regime the height difference is ~0.6 nm smaller, i.e., the height has been reduced by a factor of 1.8 (Fig. 6). Additionally, the resulting topographies differ from molecule to molecule.

The consistent decrease of the apparent height, the observation that molecules showing a Y or T shape produce the smallest apparent height of all (undisturbed) molecules, and the absence of characteristic features in the resulting images support the conclusion that repulsive interaction

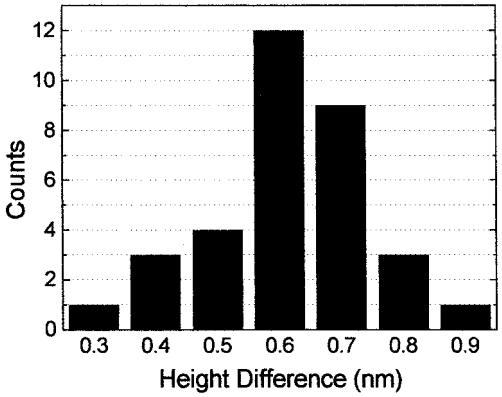

FIGURE 6 Histogram of the apparent height differences before and after the molecules were imaged in the repulsive interaction regime. In all cases, the apparent height at its maximum value has been measured from images taken in the attractive interaction regime. Each molecule has been imaged twice in the repulsive interaction regime.

regime imaging, even with relatively small free oscillation amplitudes (5 nm in some cases), implies some sort of sample damage. The multiple domain structure shown in Fig. 5 *E* could be the consequence of breaking several bonds during repulsive interaction imaging. Previously, we have verified that the apparent size of a given molecule in the attractive interaction regime is independent of the number of times this molecule has been imaged.

A detailed description of the process or processes responsible for the changes observed in the molecules is still lacking. Presently the experimental methods to measure the force exerted on the sample in tapping-mode AFM are still under development (Fain et al., 2000). Nevertheless, some insight could be gained from theoretical simulations (García and San Paulo, 1999a). Here, we have calculated the maximum tip-sample force as a function of the setpoint amplitude for a moderately compliant material ($E = 1$ GPa) and for a free amplitude, resonance frequency, tip radius, and quality factor similar to the experimental values ($A_0 = 6$ nm, $f_0 = 300$ KHz, $R = 5$ nm, and $Q = 500$).

Fig. 7 *A* shows the dependence of the oscillation amplitude on the tip-sample separation. A step-like discontinuity is observed at 4 nm. The values of the amplitude that are considered unsuitable to obtain faithful and stable images have been shadowed. Fig. 7 *B* shows the corresponding dependence of the maximum force on the amplitude. The forces applied in the repulsive interaction regime are larger than those applied in the attractive interaction regime. For example, for $A_{sp} = 5.9$ nm the maximum force is 0.4 nN, while for $A_{sp} = 2.8$ nm the force is 3.5 nN, i.e., the force is one order of magnitude higher in the repulsive interaction regime. $A_{sp} = 5.9$ nm and $A_{sp} = 2.8$ nm were the oscillation amplitudes used to obtain the images shown in Figs. 5 *A* and *B*, respectively.

Furthermore, experiments performed in air may also imply the formation of a capillary meniscus if there is tip-sample contact. Capillary forces of 10 nN are routine in AFM experiments. The force associated with the meniscus would also be exerted on the molecule. A combination of short-range repulsive forces and capillary or adhesion forces are likely the factors that contribute to the sample deformation observed in the images.

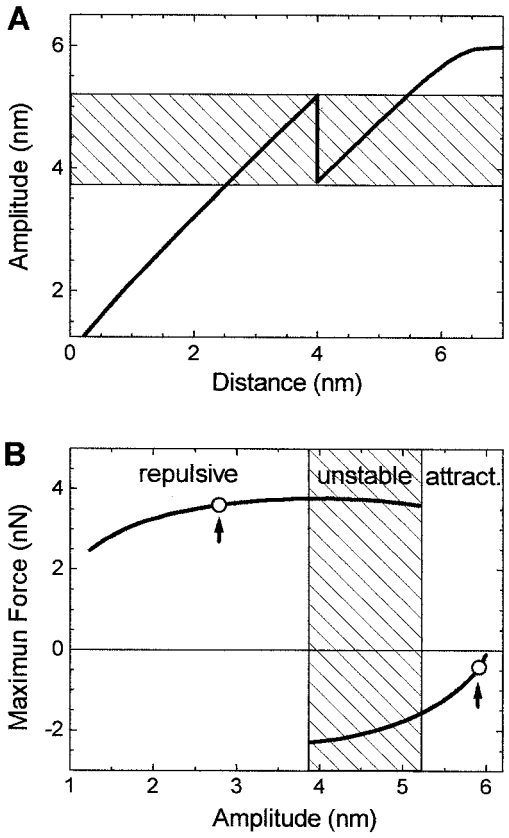

FIGURE 7 (*A*) Theoretical amplitude dependence on tip-sample separation. The shadowed region indicates the values of the oscillation amplitude that produce an unstable behavior. (*B*) Calculated maximum force dependence on the oscillation amplitude. The arrows indicate the values of the experimental setpoint amplitudes used for recording the images shown in Fig. 5.

In retrospect, it may seem hardly surprising to show that the attractive interaction regime is less disruptive than the repulsive interaction regime. The regimes were set in a way that the repulsive interaction regime involves higher forces than the attractive interaction regime. In our opinion, the above results have three far-reaching implications concerning imaging of single proteins by tapping-mode AFM. First, the attractive interaction regime is able to resolve the domain structure of proteins formed by several subunits. Second, even very gentle operation in the repulsive interaction regime may imply some kind of sample damage. Third, amplitude curves allow identification and selection of the operating regime.

Nevertheless, we do not want to convey the message that the images obtained in the repulsive interaction regime are

always associated with some sort of sample damage. Ohnesorge and Binnig (1993) were the first to demonstrate true atomic resolution in AFM by using net repulsive loading forces of 0.1 nN or lower. In fact, the relevant parameter to be considered is the actual force exerted on the sample. Relatively large attractive forces, say above 4 nN, could produce severe topographic changes in the molecules, while smaller repulsive forces, say below 0.4 nN, would not alter the molecules. We emphasize that for a given cantilever, tip radius, and free oscillation amplitude, the attractive interaction regime involves smaller forces than the repulsive interaction regime.

There are several scanning probe microscopy studies involving imaging of antibodies (Han et al., 1995; Roberts, 1995; Quist et al., 1995; Mazeran et al., 1995; Tang and McGhie, 1996; Thomson et al., 1996; Fritz et al., 1997). However, only a few of them have produced images of antibodies with a Y shape; Quist et al. reported the earliest image showing a Y shape. However, the image did not resolve the separation between domains. In the text the authors stated that only a very small amount of molecules ($\ll$1%) showed the above morphology. In our experiments $\sim$10% of the molecules appear in the Y-shaped morphology. It seems likely that most of their imaging was performed in the repulsive interaction regime, with forces high enough to disrupt the molecules.

Cryo-AFM (low temperature contact AFM) (Han et al., 1995), however, have provided images that show reproducible substructure. The combination of low applied forces and the increase of the rigidity of the molecules due to the low temperatures explain their success. In the present work we have obtained images of antibodies that are comparable in resolution to cryo-AFM images just by operating the instrument in the attractive interaction regime. No other treatment of the sample or tip was required.

This work has been motivated by some recent theoretical findings that demonstrated the existence of two different interaction regimes in tapping-mode AFM. Our purpose has been to analyze the consequences of the existence of those regimes in the imaging of single biomolecules. We have shown that imaging in the repulsive interaction regime is usually associated with a loss of contrast and resolution. In most cases the tip-sample forces present in the repulsive regime involve irreversible tip-sample damage.

The experimental results and the simulations indicate that the damage observed in images obtained in the repulsive interaction regime is due to the strength of the tip-sample repulsive forces. However, we have demonstrated that the image quality of single molecules such as antibodies, in terms of resolution and contrast, can be greatly improved by operating the AFM in the attractive interaction regime. This regime may imply very small instantaneous tip-sample forces ($<$400 pN). From a practical point of view it is important to realize that in air environments the attractive interaction regime is easily identified by the presence of a steplike discontinuity in the amplitude curves .

We are grateful to Laura Lechuga and Ana Calle for their help with sample preparation.

This work was supported by the European Commission, BICEPS, Grant BIO4-CT-2112.

REFERENCES

Allen, S., X. Chen, J. Davies, M. C. Davies, A. C. Davies, J. C. Edwards, C. J. Roberts, J. Sefton, S. J. B. Tendler, and P. M. Williams. 1997. Detection of antigen-antibody binding events with the atomic force microscope. *Biochemistry.* 36:7457–7463.

Anczykowski, B., D. Krüger, and H. Fuchs. 1996. Cantilever dynamics in quasi-noncontact force microscopy: spectroscopic aspects. *Phys. Rev. B.* 53:15485–15488.

Anselmetti, D., R. Lüthi, E. Meyer, T. Richmond, M. Dreier, J. E. Frommer, and H.-J. Güntheradt. 1994. Attractive-mode imaging of biological materials with dynamic force microscopy. *Nanotechnology*. 5:87–94.

Bustamante, C., C. Rivetti, and D. Keller. 1997. Scanning force microscopy under aqueous solutions. *Curr. Opin. Struct. Biol.* 7:709–716.

Dammer, U., M. Hegner, D. Anselmetti, P. Wagner, M. Dreier, W. Huber, and H. J. Güntherodt. 1996. Specific antigen/antibody interactions measured by force microscopy. *Biophys. J.* 70:2437–2441.

Fain, S. C., K. A. Barry, M. G. Bush, B. Pettenger, and R. N. Louie. 2000. Measuring average tip-sample forces in intermittent-contact (tapping) force microscopy in air. *Appl. Phys. Lett.* (in press).

Fritz, J., D. Anselmatti, J. J. Jarchow, and X. Fernandez-Busquets. 1997. Probing single biomolecules with atomic force microscopy. *J. Struct. Biol.* 119:165–171.

Fritz, M., M. Radmacher, J. P. Cleveland, M. W. Allersma, R. J. Stewart, R. Greselman, P. Janmey, C. F. Schmidt, and P. K. Hansma. 1995. Imaging globular and filamentous proteins in physiological buffer solutions with tapping-mode atomic force microscopy. *Langmuir.* 11: 3529–3535.

García, R., and A. San Paulo. 1999a. Attractive and repulsive tip-sample interaction regimes in tapping-mode atomic force microscopy. *Phys. Rev. B.* 60:4961–4966.

García, R., and A. San Paulo 1999b. Amplitude curves and operating regimes in dynamic atomic force microscopy. *Ultramicroscopy*. (in press).

Han, W., J. Mou, J. Sheng, J. Yang, and Z. Shao. 1995. Cryo atomic force microscopy: a new approach for biological imaging at high resolution. *Biochemistry.* 34:8215–8220.

Hansma, H., and J. Hoh. 1994. Biomolecular imaging with the atomic force microscope. *Annu. Rev. Biophys. Chem.* 23:115–139.

Haugstad, G., and R. Jones. 1999. Mechanisms of dynamic force microscopy on polyvinyl alcohol: region-specific non-contact and intermittent contact regimes. *Ultramicroscopy.* 76:77–86.

Henderson, E. 1994. Imaging of living cells by atomic force microscopy. *Prog. Surf. Sci.* 46:39–60.

Kühle, A., A. H. Soerensen, and J. Bohr. 1997. Role of attractive forces in tapping tip force microscopy. *J. Appl. Phys.* 81:6562–6569.

Lantz, M., Y. Z. Liu, X. D. Cui, H. Tokumoto, and S. M. Lindsay. 1999. Dynamic force microscopy in fluid. *Surf. Interface Anal.* 27:354–360.

Margeat, E., C. Le Grimellec, and C. A. Royer. 1998. Visualization of trp repressor and its complexes with DNA by atomic force microscopy. *Biophys. J.* 75:2712–2720.

Martin, Y., C. C. Williams, and H. K. Wickramasinghe. 1987. Atomic force microscope-force mapping and profiling on a sub 100-Å scale. *J. Appl. Phys.* 61:4723–4729.

Mazeran, P. E., J. L. Loubet, C. Martelet, and A. Theretz. 1995. Under buffer SFM observation of immunospecies adsorbed on a cyano grafted silicon substrate. *Ultramicroscopy.* 60:33–40.

Muñoz-Botella, S., M. A. Martin, B. D. Castillo, and L. Vázquez. 1996. Differentiating inclusion complexes from host molecules by tapping-mode atomic force microscopy. *Biophys. J.* 71:86–90.

Ohnesorge, F., and G. Binnig. 1993. True atomic resolution by AFM through repulsive and attractive forces. *Science.* 260:1451–1456.

Putman, C. A., K. O. van der Werf, B. G. de Grooth, N. F. van Hulst, and J. Greve. 1994. Viscoelasticity of living cells allows high resolution imaging by tapping-mode atomic force microscopy. *Biophys. J.* 67: 1747–1753.

Quist, A. P., A. A. Bergman, C. T. Reimann, S. O. Oscarsson, and B. U. R. Sundqvist. 1995. Imaging of single antigens, antibodies, and specific immunocomplex formation by scanning force microscopy. *Scanning Microscopy.* 9:395–400.

Radmacher, M., M. Fritz, C. M. Kacher, J. P. Cleveland, and P. K. Hansma. 1996. Measuring the viscoelastic properties of human platelets with the atomic force microscope. *Biophys. J.* 70:556–567.

Roberts, C. J. 1995. Real-space differentiation of IgG and IgM antibodies deposited on microliter wells by scanning force microscopy. *Langmuir.* 11:1822–1826.

Samori, B. 1998. Stretching, tearing, and dissecting single molecules of DNA. *Angew. Chem. Int. Ed.* 37:2198–2200.

Silverton, E. W., M. A. Navia, and D. Davies. 1977. Three-dimensional structure of an intact human immunoglobulin. *Proc. Natl. Acad. Sci. USA.* 74:5140–5144.

Tamayo, J., and R. García. 1996. Deformation, contact time and phase contrast in tapping-mode scanning force microscopy. *Langmuir.* 12: 4430–4435.

Tamayo, J., and R. García. 1997. Effects of elastic and inelastic interactions on phase contrast images in tapping-mode scanning force microscopy. *Appl. Phys. Lett.* 71:2394–2396.

Tang, S. L., and A. J. McGhie, 1996. Imaging individual chaperonin and immunoglobulin G molecules with scanning tunneling microscopy. *Langmuir.* 12:1088–1093.

Thomson, N. H., M. Fritz, M. Radmacher, J. P. Cleveland, C. F. Schmidt, and P. Hansma. 1996. Protein tracking and detection of protein motion using atomic force microscopy. *Biophys. J.* 70:2421–2431.

Valle, M., J. M. Valpuesta, J. L. Carrascosa, J. Tamayo, and R. García. 1996. The interaction of DNA with bacteriophage ϕ29 connector: a study by AFM and TEM. *J. Struct. Biol.* 116:390–398.

Willemsen, O. H., M. E. Snel, K. O. van der Werf, B. G. de Grooth, J. Greve, P. Hinterdorfer, H. J. Gruber, H. Schindler, Y. Van Kooyk, and C. G. Figdor. 1998. Simultaneous height and adhesion imaging of antibody-antigen interactions by atomic force microscopy, *Biophys. J.* 75:2220–2228.